International Journal of Mechanical Sciences 263 (2024) 108781

Contents lists available at ScienceDirect

International Journal of Mechanical Sciences

journal homepage: www.elsevier.com/locate/ijmecsci

Micromechanical analysis of composite materials considering material variability and microvoids

O. Vallmajó [a,*], A. Arteiro [b,c], J.M. Guerrero [a], A.R. Melro [d], A. Pupurs [e], A. Turon [a]

[a] AMADE, Polytechnic School, University of Girona, C/Universitat de Girona 4, 17003 Girona, Spain
[b] DEMec, Faculdade de Engenharia, Universidade do Porto, Rua Dr. Roberto Frias, 4200-465 Porto, Portugal
[c] INEGI, Rua Dr. Roberto Frias, 400, 4200-465 Porto, Portugal
[d] Bristol Composites Institute (ACCIS), University of Bristol, Queen's Building, BS8 1TR, UK
[e] Laboratory of Experimental Mechanics of Materials, Riga Technical university, Riga, LV 1048, Latvia

ARTICLE INFO

Keywords:
Fiber reinforced polymers (FRP)
Microvoids
Mechanical properties
Micro-mechanics

ABSTRACT

One of the main challenges for fiber-reinforced polymers (FRP) is the difficulty to predict their mechanical behavior. At the microscale, the properties of the constituents, their spatial distribution and the defects arising from manufacturing affect the mechanical behavior. In this work, statistically representative volume elements (SRVEs) are proposed based on a micromechanical finite element model to determine the effect of content, distribution and size of microstructural defects and, material uncertainties on the elastic mesoscale properties of FRPs. To that end, different cylindrical void sizes are considered as well as irregular shaped voids between fiber tows (inter-fiber voids). Fibers and voids are randomly distributed in a SRVE. An uncertainty quantification and management analysis is employed to obtain statistical descriptors of the effective mesoscale mechanical properties of FRPs. The results obtained are compared with analytical models. It is demonstrated that, for carbon fiber/epoxy composites, SRVEs with lateral dimensions equivalent to 15 times the average fiber diameter and a length of 0.01 mm along the longitudinal direction remain statistically representative with or without the presence of voids. The results show that the presence of voids reduces the transverse and shear elastic properties of FRPs. The smaller the voids are, the bigger is the reduction. Regarding the presence of inter-fiber voids, the reduction is lower. This trend is well predicted by the Mori–Tanaka mean field theory. However, the relative difference between the numerical and the analytical predictions increases for high void volume fractions. Regarding the effective longitudinal Young's modulus, the rule of mixtures, the Mori–Tanaka mean field theory and the concentric cylinder assembly model provide similar predictions for the mean value, but the uncertainty is overestimated by the analytical models because the properties of the fibers take a single value for each calculation with the analytical model, while they more realistically change from fiber to fiber in the numerical SRVEs.

1. Introduction

Composite materials are of special interest in modern industry due to their excellent specific mechanical properties. However, the brittle nature of polymer composites means that failure initiates from a stress raiser. This can be a geometrical feature, e.g., a hole, damage, e.g., impact on a surface, or the presence of defects, e.g., the existence of voids. In fiber-reinforced polymers (FRPs) there are many defects related to the constituents: fiber defects, such as fiber degradation or in-plane misalignment, matrix defects, such as porosity or contaminants, and fiber–matrix defects, such as debonding or poor wetting of the fibers [1]. Voids are among the most important defects since they affect a wide range of composite properties and they tend to be common in many different manufacturing techniques [2,3].

Voids can usually be defined as cylindrical branch-type defects generally aligned with the fiber direction [4]. The main sources of porosity in composite materials are air entrapment during the initial manufacturing stage and volatile components or contaminants generated during curing [5]. Voids may be present in a composite with different sizes, shapes and content. When studying macrovoids in carbon/carbon composites, Drach et al. [6] showed that, in unidirectional composites, assuming voids aligned with the fibers and extending continuously with constant cross-section may significantly overestimate the longitudinal and slightly underestimate the transverse stiffness of the material when compared with irregularly shaped macrovoids. On the other hand, parallel 2:1 spheroidal voids randomly distributed in the same transversely

* Corresponding author.
E-mail address: oriol.vallmajo@udg.edu (O. Vallmajó).

https://doi.org/10.1016/j.ijmecsci.2023.108781
Received 14 April 2023; Received in revised form 21 September 2023; Accepted 24 September 2023
Available online 4 October 2023

isotropic matrix result in closer predictions of the effective moduli. In the present study, however, focus will be given to the presence of voids at the level of the constituents, linked to the occurrence of porosity at the microscale. Most of the authors found, by 3D micro-CT scanning, that microvoids have a rod-like geometry oriented along the fiber direction [7–18]. Regarding the cross-section, some microvoids present an irregular shape which, for the sake of simplicity, can be fitted into a circle [17–19], whereas others are almost circular [15,20]. These microvoids typically have an equivalent diameter of 3 to 20 μm [13–16] even for thermoplastic matrices [21]. Vajari et al. [15], Hyde et al. [20] and Daggumati et al. [22] concluded that, microvoids whose size is comparable with the fiber diameter are present in a composite between fiber clusters with an irregular shape, since the matrix cannot easily flow-in during manufacturing. They also concluded that microvoids can be present as small air bubbles being trapped in the matrix.

Several studies have been focused on the effect voids have on the mechanical properties of FRPs. Experimentally, Almeida and Neto [23] determined that voids have a high detrimental effect on the fatigue life of composite structures. Chambers et al. [16] found that an increasing void content reduces the flexural strength and the fatigue performance acting on the initiation and propagation of failure mechanisms. Zhu et al. [11] concluded that cracks emanate from the voids and so both tensile strength and modulus decrease. Finally, Chu et al. [24] also observed that porosity have a detrimental effect on the transverse and shear moduli, whereas the effect on the longitudinal properties is much lower.

Accurate numerical simulations, with advanced constitutive models, can help understand the mechanical behavior at the microscale (constituents level) and their effect on the mesoscale properties (ply level). Melro et al. [25] defined a methodology to generate a micromechanical 3D representative volume element (RVE) containing randomly distributed fibers in accordance to the fiber volume fraction. Tavares et al. [26] extended this version of the random fiber generator to obtain the microstructure of a composite material with different types of fibers, i.e., a fiber-hybrid composite. In the present work, this methodology is further extended to take into account the presence of voids. To that end, an RVE of the composite material with defects needs to be defined. That is, a sample that is structurally entirely typical of the whole mixture on average and contains a sufficient number of inclusions to be effectively independent, so that the results are macroscopically uniform [27].

The analysis of the effect of matrix voids using computational micro-mechanics is not new. Previous studies include the work of Vajari et al. [15], where 2D numerical simulations were performed considering elongated voids parallel to the fiber direction with a circular cross section. Inter-fiber voids with an irregular shape were also considered. Dong [28] studied the effect of randomly distributed voids on the stiffness and strength of FRP also comparing the results with analytical models. Mehdikhani et al. [2,18] also simulated the effect of microvoids on the elastic moduli of carbon fiber reinforced polymers considering a single ellipsoidal void embedded in the matrix. These voids will be simply referred to as ‘‘matrix voids’’. Hyde et al. [14,20] used a micromechanics-based finite element modeling strategy to study the effect of a single matrix or inter-fiber void on the strength of composite structures. Sharifpour et al. [29] developed a 2D micromechanical model to assess the effect of microvoids on the local stress state, with a circular shape, in a cross-ply laminate. Chu et al. [24] studied the influence of voids on the stiffness properties of unidirectional FRPs, considering very small spherical voids. More recently, Daggumati et al. [22] checked the effect of matrix and inter-fiber voids, as well as other geometrical and material features such as thermal residual stresses and the random spatial distribution of the reinforcements, in a 2D cell under a transverse loading state. Vinot et al. [30] developed a model to quantify uncertainties, e.g., porosity, in continuous unidirectional composites and evaluate their influence on the mechanical properties of the material. However, to the authors’ best knowledge, all the current literature studies have not taken into account simultaneously the random spatial distribution of the constituents, the variability in their properties and the variability of the characteristics of microvoids in the definition of statistically representative volume elements (SRVEs) for fiber-reinforced polymers.

In the design of composite structures it is also important to take into account the uncertainties in the design parameters, arising, for example, from the scatter in the material properties. Vallmajó et al. [31] defined a methodology to account for the uncertainty of an open-hole specimen by calculating analytically B-value design allowables through Monte Carlo simulation (MCS). The B-value is a statistically-based design allowable, recommended by the Composite Materials Handbook (CMH-17) [32], and defined as the 95% lower confidence bound on the tenth percentile of a specified population of measurement. Cózar et al. [33] also created a methodology to calculate the B-value from a high-fidelity numerical model creating a response surface of the results and, afterwards, performing a MCS. These strategies rely on input material properties at the ply level, and their uncertainties, characterized by experimental results to, finally, obtain the B-value allowables. However, contribution to uncertainty is not only based on the scatter in the material properties, but also from the presence of defects and their characteristics. Currently, there is a lack of studies considering the definition of SRVEs that, besides the random distribution of the reinforcements, also take into account the uncertainty of the material properties as well as the presence of defects. Therefore, SRVEs are generated herein that account for the effect of the uncertainties related to void content, distribution and size, and for the effect of the uncertainties of material properties on the elastic mesoscale properties of a carbon fiber reinforced polymer (CFRP). The methodology proposed in this work can be used to guide the quantification of uncertainties at the micro-scale, for example, to help defining knock-down factors for the effect of voids and void content, or to generate statistically representative material allowables to be used in analysis methods at the meso and macroscales. Rather than simply providing deterministic predictions of effective properties (and strengths), this methodology will enable the calculation of reliable statistical descriptors, herein focused on the effective elastic properties, but with the possibility to be extended to the stochastic prediction of damage initiation and propagation. This first step considering only the effective elastic properties will allow the assessment of the proposed approach with alternative methods, incl. well established analytical models.

The paper is organized as follows: Section 2 shows the methodology followed to generate, simulate and post-process the results from an RVE with the presence of defects; Section 3 describes the composite material and defects considered in this study; Section 4 presents the results and their discussion; finally, Section 5. summarizes the conclusions of this work.

2. Methodology

In this work, an exhaustive methodology is proposed to define SRVEs and determine the elastic properties of FRPs accounting for the uncertainty due to the material and geometric variability in the constituents, their spatial distribution and the presence of defects, in the form of matrix and inter-fiber voids. The flow chart in Fig. 1 shows the uncertainties propagation procedure followed in this study, as described in the following sections.

2.1. Composite microscopic uncertainties

In previous studies addressing the effect of the presence of microvoids on fiber-reinforced composite systems [2,8,22,24,34], the determination of the elastic properties did not account for the uncertainties associated with the intrinsic variability of the constituent properties, their spatial distribution and the characteristics of this class of defects.

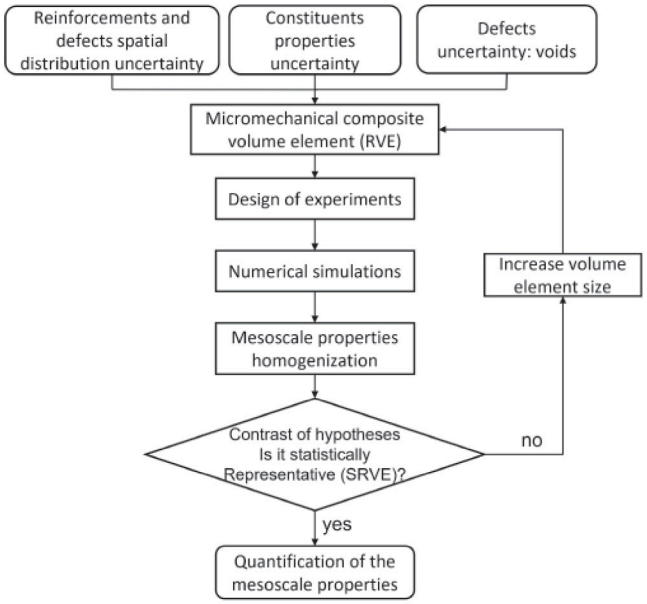

Fig. 1. Flow chart of the propagation of the uncertainties related to a composite structure to quantify their effect on the elastic mesoscale properties of the composite.

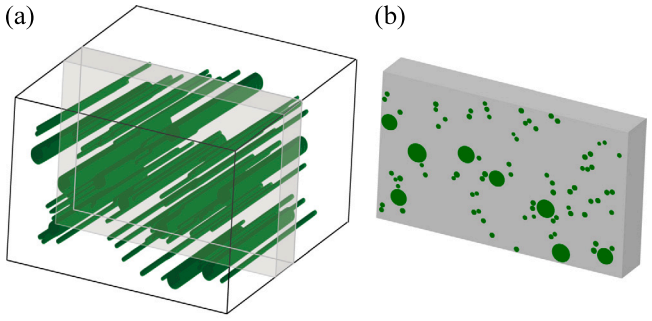

Fig. 2. A schematic 3D representation of voids inside a unidirectional ply obtained from micro-computed tomography in the literature [7,17,18,21] (a) and the corresponding representative volume element considered in this study (b).

2.1.1. Reinforcement and defects spatial distribution uncertainty

The reinforcements of FRPs are randomly distributed inside a ply. In addition, the distribution of the defects also does not follow a deterministic dispersion. Therefore, their random spatial distribution is taken into account in this study when generating the micromechanical model.

2.1.2. Constituent properties uncertainty

The different materials present in a composite system exhibit an intrinsic variability in their properties. Moreover, the size of the fibers are not constant. Therefore, the variability in the properties of the constituents and in their geometrical parameters, such as the fiber diameter, is taken into account in this study to quantify the elastic material properties of the composite.

2.1.3. Defects uncertainty: Voids

In the present work, following the data available from the literature (see Section 1), all voids are assumed to be aligned with the fiber direction (see Fig. 2).

Looking to the literature, most authors agree that voids can be represented with a circular cross-section. Moreover, in this study optical microscopy images were analyzed to characterize typical voids in

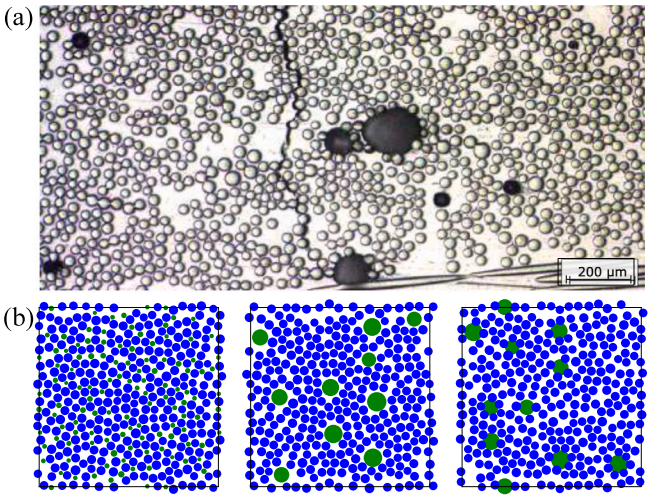

Fig. 3. (a) Image from optical microscopy with the presence of voids in dark color and (b) the corresponding RVEs (in blue the fibers and the white region is the matrix) with the presence of three types of voids (in green). From left to right: matrix voids with a diameter smaller than the fibers ("small" matrix voids), matrix voids with a larger diameter ("large" matrix voids) and voids that intersect with the fibers (inter-fiber voids). (For interpretation of the references to color in this figure legend, the reader is referred to the web version of this article.).

glass/epoxy cross-ply laminates manufactured using pre-preg lay-up. Optical microscopy images were taken observing polished specimen edges with magnification of 200x. It is assumed that the typically observed shape and distribution of voids in glass/epoxy composite shown in Fig. 3a also applies for carbon/epoxy composites analyzed in this study. The images support that porosity appears as voids with a circular shape entrapped in matrix-rich regions or as voids with an irregular shape within the fiber tows. Therefore, this study is focused on these two types of voids: matrix voids and inter-fiber voids. Moreover, in addition to the position of the voids, the effect of their size is also considered. According to the size, voids could be classified as voids with a diameter smaller than the fibers (small matrix voids) or voids with a larger diameter (large matrix voids), as shown in Fig. 3b. It is important to note that, in this study, "small" and "large" voids (Fig. 3b) refer simply to the relative size of the voids when studying the influence of their size (considering the relative size of the fibers just as a reference), and not to an absolute measure.

Void content is calculated as the void volume fraction in FRPs, e.g., following the ASTM D2734 standard that compares the theoretical and the measured composite density [35]. Although porosity should not exceed 1% for high-performance laminates and a void content greater than 5% for a composite is not acceptable in most industries, this work addresses void contents ranging up to 10% to characterize their effect in a wider range, including some of its highest and critical values reported in the literature [14,17,24,36].

2.2. Micromechanical model with voids

In the following, the approach followed to generate the micromechanical finite element model including all uncertainties taken into account in this study, described in Section 2.1, is summarized.

Generation of an RVE. The micromechanical model proposed by Melro et al. [25] to randomly distribute the fibers in an RVE and extended by Tavares et al. [26] to be able to define different types of fibers was modified to accurately represent an RVE with voids. The algorithm has been enhanced to generate voids with cylindrical shape parallel to the fiber direction, randomly distributed in the RVE. Two different populations are defined. The first one represents the fibers with its own geometrical properties, uncertainties and volume fraction. The second

population includes the voids, which also have their own properties and uncertainties.

The algorithm consists of the following steps:

1. Hard-core model to randomly distribute the constituents in the RVE. Therefore, in this first step, the model simply generates randomly new fibers and voids in the RVE. These are accepted on the RVE depending on a distance criterion that checks if these overlap with other fibers or voids. This criterion is different for fibers and voids as will be clarified later.
2. First Heuristic to move closer the fibers and voids between them to gain more empty areas to fill afterwards.
3. Second Heuristic to move the constituents on the outskirts towards the center of the RVE and compact them for generating matrix-rich regions.

The use of the heuristics allows reaching fiber volume fractions over 65% [25]. After these steps, the model starts a new iteration and repeats all the steps to add more fibers and voids until the desired volume fraction is achieved. In-deep details about these steps can be found in Ref. [25]. Overall, the model has the following abilities:

- Adding either fibers or voids according to the RVE size and their volume fractions.
- Defining a mean value and standard deviation for the diameters of the fibers and voids to account for the uncertainties related to their size.
- Defining three different minimum distances while placing the fibers and voids. One between fibers, another between fibers and voids and, finally, between voids. Thus, the algorithm can generate different types of voids: voids embedded in matrix-rich regions or inter-fiber voids which overlap with the fibers. These distances are defined as the mean radius of two consecutive circles of radius r_i and r_{i+1}, respectively, multiplied by a different constant value (k) for each minimum distance previously described ($k_{\text{fiber}-\text{fiber}}$, $k_{fiber-void}$ and $k_{void-void}$, respectively). Hence, the minimum distance between two of these features is calculated as $k \times (r_i + r_{i+1})/2$. For the case of inter-fiber voids, the distance between fiber and void is negative to allow the overlap between them, thus $k_{fiber-void} < 0$. Instead, for the matrix voids, this distance must be larger than 0 since no overlap is permitted.
- Generating fiber-rich regions (fiber clusters) where fibers are more compacted.

Thus, different categories of RVEs with voids can be generated (see Fig. 3) to assess the effect of shape and size of the voids, for example: (i) matrix voids with a diameter smaller than the fibers (small matrix voids); (ii) matrix voids with a diameter larger than the fibers (large matrix voids); (iii) voids that intersect the fibers (inter-fiber voids).

To avoid the appearance of zero-volume elements when meshing the RVE, the algorithm was modified to force that fibers and voids close to the boundaries of the RVE remain, at least, at a distance from the boundaries equal to the average size of the matrix finite elements. Likewise, the fibers and voids cut by the RVE boundaries are cut, at least, at a section as large as their corresponding mesh size.

Modeling strategy. Once the RVE is generated according to the size, fiber volume fraction, void volume fraction and their respective diameters and variation, it needs to be discretized and analyzed using the Finite Element Method (FEM). Fig. 4 shows the sequence of steps used to generate the FEM model of the RVE. It can be summarized as follows:

(a) Creation of each part, i.e., each fiber, each void and the matrix, independently as a plate, i.e., in two dimensions (2D).
(b) Assembly of all the plates and mesh of the whole model, with the possibility of defining a different mesh size for each constituent (fiber, matrix and defect). The element mesh shape is defined as quad-dominated. Thus, almost all the elements are quadrangular except in some regions where triangular elements are included. Linear elements with reduced integration are used.

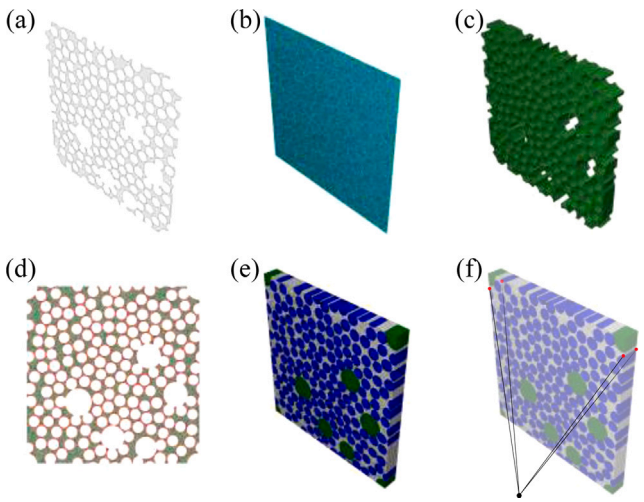

Fig. 4. Steps to model the RVE: (a) creation of each part as a plate, (b) assembly of all the parts and meshing, (c) extrusion of the mesh and conversion to 3D parts, (d) creation of each surface to define the contacts between materials, (e) assembly of all 3D parts, and (f) example of application of the periodic boundary conditions in a specific node linked with the dummy node where the far-field strains are applied.

(c) Extrusion of the mesh to convert each plate to a three-dimensional (3D) part. This strategy is followed to ensure that there is a mesh continuity in the longitudinal direction as done in previous works [34]. Hence, the periodic boundary conditions can be implemented afterwards without any problem. After the extrusion, the majority of the elements are C3D8R which correspond to linear brick elements with reduced integration, whereas in some regions the elements are C3D6 which correspond to linear triangular prism elements.
(d) Determination of each surface from each 3D part to define the constraints between the materials.
(e) Assembly of all 3D parts. The fibers and the matrix are connected with contact interactions, which adds the possibility of representing fiber–matrix debonding by employing cohesive surfaces, while the voids are assumed to be perfectly bonded to the matrix and fibers by defining contact interactions with a high penalty stiffness. It should be noted that tie constraints cannot be used since this would lead to over-constraining some nodes (the ones in the boundaries) with more than one equation: one for the periodic boundary conditions and another for the tie constraints.
(f) Implementation of the periodic boundary conditions (PBC) to link nodes in opposite faces, edges or vertices, while the micromechanical model is generated to guarantee that the RVE is geometrically and materially periodic [37]. In other words, if a fiber crosses the boundary of an RVE, the external part must be cut and moved to the opposite side keeping the same material properties. Thus, the periodicity of stress/strain field is ensured. A set of constraint equations is defined between all the nodes at the boundaries of the RVE along all degrees of freedom, through a dummy node where the far-field strain is applied (see Fig. 4f). For the complete set of equations defining the PBC, the reader is referred to Ref. [37]. To prevent rigid body motion (RBM) a random node in the middle of the RVE is fixed.

2.3. Design of experiments

Once the micromechanical RVE is created, the uncertainty of the input parameters, i.e., the variability in the constituents, the random spatial distribution and the presence of voids, is propagated to the mesoscale elastic properties (engineering constants) to quantify their

effect. To that end, an MCS is carried out. The MCS relies on the repetition of random samples to obtain statistically relevant results. In other words, a sample with n RVEs is created, where each RVE has different material properties, random spatial distribution of the constituents and random distribution of the different types of voids, and it is analyzed to obtain the distribution of the homogenized elastic material properties. The constituent properties are generated following a statistical distribution. In each RVE, the fibers are generated with different dimensions and properties according to their input distributions. The matrix properties also change, but from RVE to RVE, according to their corresponding input distributions.

2.4. Numerical simulation

The micromechanical model is simulated using the finite element software ABAQUS/Standard 6.14–2 [38]. To determine the effective elastic properties of the composite system, far-field strains of 0.001% were applied, and the stress and strain fields in the RVE post-processed (see Section 2.5).

2.5. Mesoscale properties homogenization

The uncertainties present in composite systems may be taken into account while predicting the elastic properties. According to the CMH-17 [32], the elastic properties should be defined with its mean and standard deviation. Therefore, from each simulation, the elastic properties of a composite material and their corresponding uncertainty are determined using a first-order homogenization technique (more details in Appendix A).

The results of the computational micromechanics model obtained from first-order homogenization are compared with the results calculated analytically using the rule of mixtures (RoM), the Mori–Tanaka theory and the concentric cylinder assembly (CCA) model. The RoM provides reasonable values for the longitudinal stiffness assuming that the fibers and the matrix are working in parallel, and assuming that the fibers and matrix are working as springs in series for the transverse and shear properties (more details in Appendix B). However, the predictions using the RoM for the transverse and shear stiffness are not accurate. Therefore, other micromechanical models have been proposed in the literature to determine these properties, such as the Halpin–Tsai [39] model. But to account for the presence of multiple types of inclusions (here fibers and voids), the elastic properties are better estimated using the Mori–Tanaka mean field theory [40] (more details in Appendix C). Finally, the CCA model [41] is also checked since it also allows the presence of multiple phases (more details in Appendix D).

The uncertainty quantification analyses performed numerically using computational micromechanics and analytically following the RoM, the Mori–Tanaka mean field theory, and the CCA model are compared, in terms of the obtained mean values and STDVs. The comparison considers the constituent properties variability in all cases, and includes the spatial distribution of the reinforcements and of the defects in the case of computational micromechanics (the only one herein that can account for these effects).

2.6. Definition of statistically representative volume elements (SRVEs)

The definition of an RVE implies that the results obtained are macroscopically uniform. That is, the RVE must be large enough to be representative of the continuum at a higher scale. Thus, an infinitesimal RVE may be used. However, in numerical analysis a finite size is required [42]. On the other hand, SRVEs must reproduce the same statistics related to the stress and strain fields of the macroscopic material. To account for the spatial distribution of constituents and defects and the possible material variation, a number of samples (n) is analyzed to determine these statistics.

To determine the minimum size of the SRVE, the mean values of the properties of interest obtained with volume elements of different size and discretization options (type and size of the finite elements) are determined and compared. A contrast of hypotheses is performed to check if two means can be assumed to be equal:

$$\begin{aligned} H_0 &: \bar{x_1} = \bar{x_2} \\ H_1 &: \bar{x_1} \neq \bar{x_2} \end{aligned} \tag{1}$$

where H_0 and H_1 are the null and alternative hypotheses assuming that $\bar{x_i}$ is the mean value of each sample. A pooled standard deviation, S_p, is used as an estimator of common population standard deviation:

$$S_p = \sqrt{\frac{(n_1-1)s_1^2 + (n_2-1)s_2^2}{n_1+n_2-2}} \tag{2}$$

where n_i is the sample size and s_i the standard deviation of each sample. Using the S_p and the $\bar{x_i}$ of the main data set and the ones to be compared, the test statistic

$$t_0 = \frac{\bar{x_1} - \bar{x_2}}{S_p - \sqrt{\frac{1}{n_1} + \frac{1}{n_2}}} \tag{3}$$

is used to determine if the null hypothesis can be accepted or if it must be rejected. Since this is a two-sided t-test, the required t value to accept the null hypothesis, i.e., the mean values are equal, is:

$$t_{a,n} = t_{\frac{\alpha}{2}, n_1+n_2-2} \tag{4}$$

where α is the probability of rejecting the null hypothesis when it is true. Finally, the p-value, which is the probability of obtaining test results outside the results observed under the assumption that the null hypothesis is true, is calculated. Therefore, the p-value to accept H_0 must satisfy that:

$$\text{p-value} = P(t_0 \leq t_{n_1-n_2-2}) \geq \alpha \tag{5}$$

Moreover, in this study, the variance in the results due to the uncertainty of the input parameters, such as the material variability, the spatial distribution and the presence of defects, is an important parameter that must be independent of the SRVE size and discretization. Thus, to determine the parameters for generation of SRVEs, a contrast of hypotheses is also performed to ensure that the standard deviations (STDVs) are independent of the modeling options:

$$\begin{aligned} H_0 &: s_1 = s_2 \\ H_1 &: s_1 \neq s_2 \end{aligned} \tag{6}$$

The test statistic used to determine if the null hypothesis can be accepted is F_0 defined as:

$$F_0 = \frac{s_1^2}{s_2^2} \tag{7}$$

Since this is an F-test, the F_{n_1-1,n_2-1} statistic is used to accept the null hypothesis, i.e., that the STDVs are equal. Thus, the p-value can be calculated as:

$$\text{p-value} = P(F_0 \leq F_{n_1-1,n_2-1}) \geq \alpha \tag{8}$$

So, the minimum size of the SRVE is determined by the one that provides the same mean values and STDVs of a larger one.

3. Composite material selection and effect of defects

This section describes the properties of the constituents, i.e., fibers and matrix, and the characteristics of the defects, i.e., voids, which will be used to determine the effect of defects on FRPs.

Table 1
Mean values of the elastic properties of the constituents and assumed standard deviations (STDVs).

Constituent	E_1 [MPa]		E_2, E_3 [MPa]		ν_{12}, ν_{13}		ν_{23}		G_{12}, G_{13} [MPa]		G_{23} [MPa]	
	Mean	STDV	Mean	STDV	Mean	STDV	Mean	STDV	Mean	STDV	Mean	STDV
Carbon fiber AS4	225 000	11 250	15 000	750	0.2	0.01	0.07	0.0035	15 000	750	7000	350
Epoxy matrix 3501/6	4200	210	–	–	0.34	0.017	–	–	1567	78.35	–	–

Table 2
Mean and STDV of the void diameter and the distance between fibers and voids, defined as $k_{void-fiber}$ multiplied by the mean radius, for each type of void analyzed in this study.

Void type	Mean diameter [mm]	STDV diameter [mm]	$k_{fiber-void}$ [–]
Small matrix voids	0.004	0.0004	0.1
Large matrix voids	0.014	0.001	0.1
Inter-fiber voids	0.014	0.001	−0.05

3.1. Properties of the constituents

The proposed methodology can be applied to any FRP. In this study, the material system considered is composed of AS4 carbon fibers embedded in a 3501-6 epoxy matrix. The properties of the constituents are summarized in Table 1 [43]. However, the material properties variability has not been previously reported. Other studies, such as [44], which accounted for the uncertainty in the predicted mechanical properties and the failure strengths of composite laminates, also assumed a variation equivalent to 5% of the mean value for the properties of the constituents. Moreover, the CMH-17 [32] suggests defining the elastic properties with its mean and standard deviation. So, in this analysis, a normal distribution of the material properties is considered, with a coefficient of variation of 5%.

In this study, the fiber–matrix interface is assumed to be perfectly bonded. Thus, using the interaction properties in ABAQUS/Standard, a surface interaction between fibers and matrix is used with a high penalty stiffness and without taking damage into account (i.e., without interface degradation).

The fibers have a cylindrical shape with a mean diameter of 0.007 mm and a STDV of 0.0003 mm according to Ref. [45]. The minimum distance between them ($k_{\text{fiber}-\text{fiber}}$) is defined as 0.1 times the mean radius of the two adjacent fibers. Due to the presence of voids, the fiber volume fraction (V_f) tends to be lower than usual. Therefore, the fiber volume fraction considered in this study is 55%, i.e., it is kept constant with a value of 55% while the matrix volume fraction (V_m) is reduced according to the void volume fraction (V_v).

The dimensions of the RVE and the mesh size are determined according to the statistical analysis explained in Section 2.6 and developed in Section 4.1.

3.2. Distribution and discretization of defects

As discussed previously (see Sections 1 and 2.1.3), at the microscale, voids can be represented with a cylindrical shape parallel to the fiber direction (longitudinal direction) with a circular cross-section (matrix voids), whereas inter-fiber voids present an irregular shape due to their intersection with the fibers.

The generation of voids in the finite element model is performed according to the assigned diameter and void content. Although most industries do not allow void contents above 5%, the void volume fraction considered in this study is 7% to promote a greater influence and characterize more clearly their effect, a similar approach to previous studies [14,24,28]. The characteristics of each type of voids analyzed in this study is summarized in Table 2. The minimum distance between voids ($k_{void-void}$) is two times the mean radius of two consecutive voids to allow to have fiber bundles around them.

For the sake of simplicity, and since all the SRVEs analyzed in this study are only a small portion of the whole ply (see Fig. 2b), voids represented in this micromechanical model extend along the length the SRVE, although it is recognized that, unlike the fibers, voids are not continuous. Yet, given their rod-like geometry, this is considered a suitable approximation.

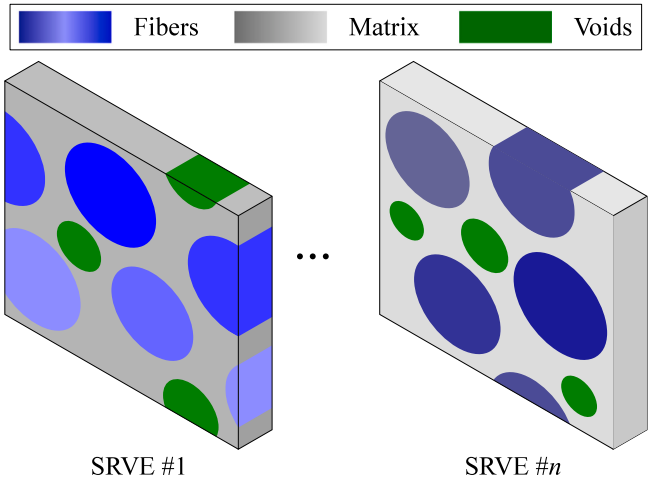

Fig. 5. Illustration of two SRVEs containing small matrix voids. The different grades of the colors show the material variability of the matrix between samples and of the fibers in each sample. Material periodicity is ensured. Geometrical variability of the fibers and voids is also represented. (For interpretation of the references to color in this figure legend, the reader is referred to the web version of this article.).

Voids dummy material. Voids represent air entrapped in the composite system. To avoid numerical problems and account for the volume variation of the RVE due to the elastic deformations, in this study voids are characterized using an isotropic dummy material [2]. A parametric analysis was conducted to assess the effect of the dummy material properties on the resulting homogenized composite properties. Finally, a value equal to 0.001 MPa for the Young's modulus and 0.001 for the Poisson's ratio resulted in no effect on the homogenized composite properties.

4. Results and discussion

This section presents, the statistical analysis to determine the SRVE, the effect of voids on FRPs and the discussion of the results obtained in this study.

4.1. Determination of the minimum size of the SRVE

A sample size n of 20 samples is analyzed. In each sample, all different fibers have random material and geometric properties according to their respective normal distribution, whereas voids have different dimensions according to their associated uncertainty. Each model also has different material properties for the matrix and a random spatial distribution of the fibers and of the defects. Therefore, each sample takes into account the material variability, the geometrical uncertainties, the effect of voids and the random spatial position of the fibers and defects (see Fig. 5).

To determine the minimum size of the SRVE and its most efficient discretization, a contrast of hypotheses for the means and the STDVs with a significance level of 5% ($\alpha = 5\%$) is performed. The parameters studied in this statistical analysis are:

Table 3
Contrast of hypotheses of the mean value ($H_{0,mean}$) and the STDV ($H_{0,STDV}$) of a 15 × 15 model to determine the minimum mesh size for discretization of fibers and matrix. The values in **bold** are the reference values used for the contrast of hypotheses.

Matrix finite element size	Fiber finite element size	
	0.00035 [mm]	0.00070 [mm]
0.00035 [mm]	**Ref value**	$H_{0,mean}$: False for E_1 $H_{0,STDV}$: False for G_{23}
0.00070 [mm]	$H_{0,mean}$: True $H_{0,STDV}$: True	$H_{0,mean}$: False for E_1, E_2, G_{12}, G_{23} $H_{0,STDV}$: True

1. The length on the longitudinal direction of the SRVE.
2. The mesh size. The fibers and the matrix can have different mesh sizes.
3. The size of the SRVE (width and height) considering a square cross-section. The SRVE size is determined relative to the fiber diameter, i.e., if the SRVE width is 20, that means that the width and height will be 20 times the mean fiber diameter (0.007 mm).
4. The presence of defects, i.e., whether the size of the SRVE is affected by the presence of voids.

Determination of the minimum length. To determine the minimum length of the SRVE, three different lengths are analyzed: 0.1 mm, 0.05 mm and 0.01 mm, in line with previous numerical studies [46]. Moreover, three model sizes were analyzed: 5 × 5, 10 × 10 and 15 × 15, corresponding to a width and height 5, 10 and 15 times the mean fiber diameter (0.007 mm), respectively. For this analysis, the size of the finite elements was 0.0007 mm. The RVE with a length equal to 0.1 mm is taken as the reference.

The contrast of hypotheses, for the mean and STDV, were true for all the cases analyzed. It can be concluded that the length has no effect when determining the elastic properties since, for any length and size, the mean value and the STDV can be assumed to be equal to the reference value (0.1 mm long RVE). SRVEs with a length of 0.01 mm are, therefore, chosen, discretized by 5 elements, leading to a mesh size in the longitudinal direction of 0.002 mm.

Determination of the mesh size. To perform the mesh convergence study, four different mesh sizes according to the fiber diameter were evaluated in an RVE with a model cross-section of 15 × 15 fibers. The reference one is the finest, which has an element size of 0.00035 mm for both the matrix and the fibers. This leads to approximately 20 elements across the fiber diameter. Moreover, different combinations of mesh sizes for the matrix and the fibers are considered. Fig. 6 shows the results for the four different mesh size combinations normalized by the reference value. Table 3 summarizes the results of the contrast of hypotheses for the mean values and the STDVs for the mesh convergence study.

From the results of the contrast of hypotheses, the fibers will be discretized by finite elements with 0.00035 mm whereas the matrix will be discretized by finite elements with 0.00070 mm, very close to the values obtained by Li et al. [47], without compromising the accuracy of the results. The use of a heterogeneous mesh enables reducing the total number of elements and the computational cost with respect to the finest mesh attempted.

Determination of the SRVE size. Once the length of the SRVE has been determined to be 0.01 mm and the mesh size 0.00035 mm for the fibers and 0.00070 mm for the matrix, finally, the cross-section size of the SRVE is studied. Four possible SRVE sizes were studied. The reference has 20 × 20 fibers. The results are shown in Fig. 7. The study of the contrast of hypotheses is summarized in Table 4.

From this statistical analysis, it can be concluded that the reference value previously selected (20 × 20) is representative since the contrast of hypotheses demonstrate that there is a smaller RVE (15 × 15) with the same mean and STDV for all the elastic properties. So, a convergence of the results is achieved. Therefore, to not compromise the computational time and resources needed, the SRVEs with a cross-section size of 15 × 15 fibers, i.e., 0.105 mm width and 0.105 mm height, are selected. These values are in good agreement with some other studies available in the literature. For example, Trias et al. [42] determined that the minimum size should be between 5 × 5 and 25 × 25 fiber diameters. Moreover, it is also in good agreement with González and Llorca [48] who predicted that an RVE with 30 fibers is representative of the macroscopic material. In the present study, with a 15 × 15 cross-section, the number of fibers is much larger than 30.

Table 4
Contrast of hypotheses of the mean value ($H_{0,mean}$) and the STDV ($H_{0,STDV}$) for different model dimensions to determine the smallest SRVE assuming a length of 0.01 mm and a mesh size of 0.00035 mm for the fibers and 0.00070 mm for the matrix. The values in **bold** are the reference values used for the contrast of hypotheses.

SRVE	$H_{0,mean}$	$H_{0,STDV}$
Cross-section size 20 × 20	**Ref value**	**Ref value**
Cross-section size 15 × 15	True	True
Cross-section size 10 × 10	True	False for E_1
Cross-section size 5 × 5	False for G_{12}, G_{23}	False for E_1

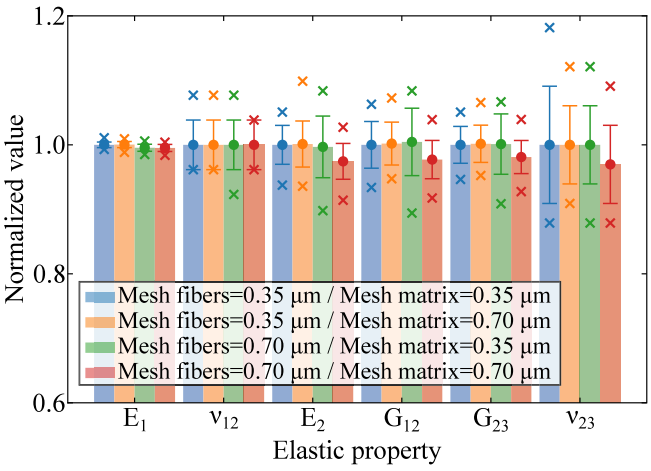

Fig. 6. Normalized elastic properties from a cross-section size 15 × 15 with four different mesh sizes for the fibers and the matrix. The crosses are the minimum and maximum values, and the circle the mean value with an error bar equal to one STDV. (For interpretation of the references to color in this figure legend, the reader is referred to the web version of this article.).

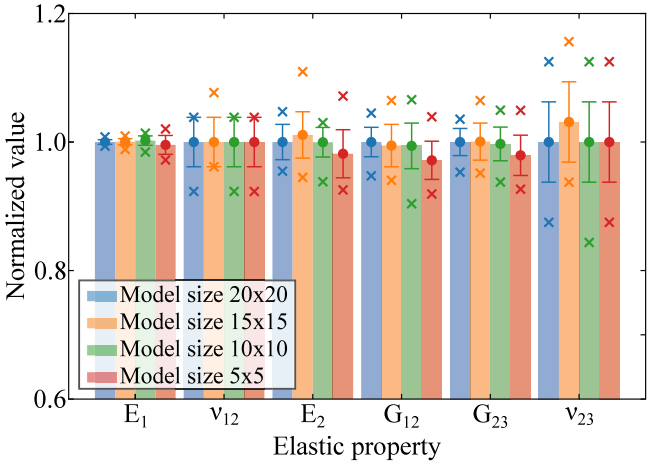

Fig. 7. Normalized elastic properties from 5 × 5, 10 × 10, 15 × 15 and 20 × 20 cross-section size to determine the minimum size. The crosses are the minimum and maximum values, and the circle the mean value with an error bar equal to one STDV. (For interpretation of the references to color in this figure legend, the reader is referred to the web version of this article.).

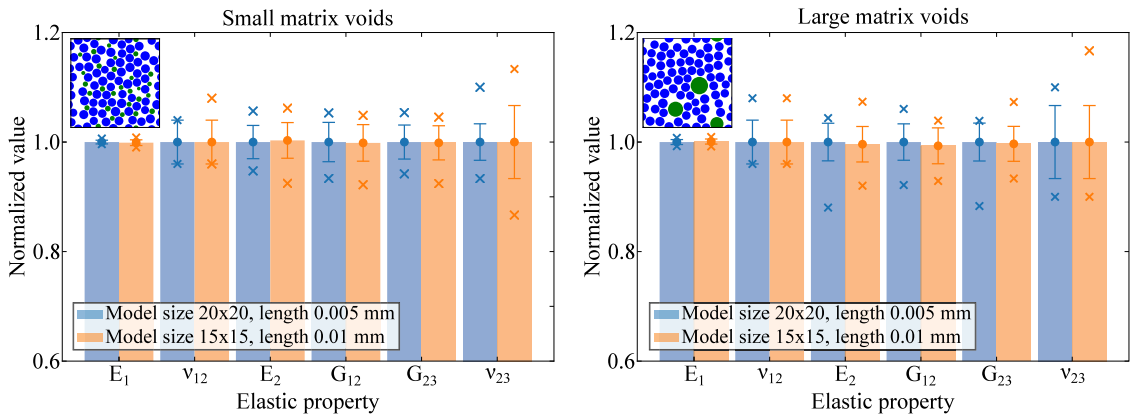

Fig. 8. Normalized elastic properties with the presence of matrix voids. The crosses are the minimum and maximum values, and the circle the mean value with an error bar equal to one STDV. (For interpretation of the references to color in this figure legend, the reader is referred to the web version of this article.).

Table 5
Contrast of hypotheses of the mean value ($H_{0,mean}$) and the STDV ($H_{0,STDV}$) to determine the effect of the presence of voids on the model size. Two RVEs with voids have been analyzed: small matrix voids and large matrix voids. The values in **bold** are the reference values used for the contrast of hypotheses.

SRVE	20 × 20 in plane size L = 0.05 mm	15 × 15 in plane size L = 0.01 mm
Small matrix voids	**Ref value**	$H_{0,mean}$: True $H_{0,STDV}$: False for ν_{23}
Large matrix voids	**Ref value**	$H_{0,mean}$: True $H_{0,STDV}$: True

To sum up, for a sample size of 20 SRVEs, the minimum lateral dimensions are 15 × 15 fibers, with a mesh size of 0.00035 mm for the fibers and 0.00070 mm for the matrix and a length in the longitudinal direction of 0.01 mm. With this combination, the number of finite elements for each SRVE is around 450 000.

Verification of the SRVE size with the presence of voids. The previous analyses, performed on "pristine" microstructures, is now repeated considering the presence of voids. The 20 × 20 RVEs with a length of 0.05 mm and matrix voids are taken as reference and compared with the previously determined: 15 × 15 fiber diameters cross-section and a length of 0.01 mm. In both cases, the mesh size for the fibers is 0.00035 mm, whereas for the matrix and the voids the mesh size is 0.00070 mm, which correspond to the best mesh combination found previously. The results of the elastic properties normalized by the reference values are shown in Fig. 8, while Table 5 summarizes the results from the contrast of hypotheses for the mean values and the STDVs.

From the contrast of hypotheses, independently of the size of the matrix voids, the mean values can be considered statistically equivalent, while for small matrix voids the STDV of ν_{23} cannot. This is explained by the presence of two extremely high values (see the corresponding minimum and maximum value in Fig. 8) in two of the 20 samples with small matrix voids. Neglecting these two extreme results, the STDVs turn out statistically equivalent.

Based on these results, it can be concluded that the size of the SRVE previously selected is practically independent of the presence of voids.

4.2. Effect of voids on the elastic properties

Finally, once the characteristics of the SRVE have been determined, the elastic engineering constants are calculated with the presence of voids. Different types of voids are analyzed, including matrix voids and inter-fiber voids to assess the effect of voids shape and size. For reference, SRVEs without defects or material variability and SRVEs without defects and material and geometric variability are also considered. The results are shown in Fig. 9.

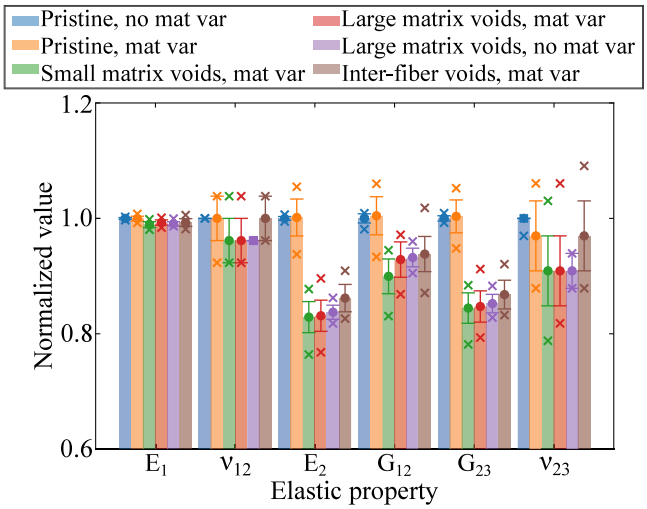

Fig. 9. Normalized engineering constants obtained from six different SRVEs: (i) without defects (pristine) and without material variability, (ii) without defects (pristine) but with material variability, (iii) with small matrix voids and material variability, (iv) with large matrix voids and material variability, (v) with large matrix voids but without material variability and (vi) with inter-fiber voids and material variability. All models account for the spatial variability of the fibers (and voids). The crosses are the minimum and maximum values, and the circle the mean value with an error bar equal to one STDV. (For interpretation of the references to color in this figure legend, the reader is referred to the web version of this article.).

As expected, the presence of voids implies a reduction of the elastic properties, and the transverse and shear properties experience the highest reductions. Pristine SRVEs without material or geometrical variability exhibit very low variability of their elastic properties since they only account for the random spatial distribution of reinforcements. However, when introducing material and geometrical variability, the STDV increases without major changes in the mean values of the elastic properties. Interestingly, the presence of voids reduced the mean value of the elastic properties, but the variability (STDV) is barely affected. To check the effect of voids on the STDV, a set of analyses with large matrix voids but without material variability was performed. The results show that the mean value is almost the same, whereas the variability is smaller when only taking into account the uncertainty

Table 6
Effect of the presence of voids on the elastic properties of a composite system. The cases with voids include material variability.

Elastic property		No material variability No defects	Material variability No defects	Small matrix voids	Large matrix voids	Large matrix voids No material variability	Inter-fiber voids
E_1 [MPa]	Mean	125 760	125 714	124 385	124 853	124 560	124 848
	STDV	182	511	651	577	471	842
	Rel. dif.	–	−0.04%	−1.09%	−0.72%	−0.95 %	−0.73%
ν_{12} [–]	Mean	0.26	0.26	0.25	0.25	0.25	0.26
	STDV	0.0	0.01	0.01	0.01	0.01	0.01
	Rel. dif.	–	0%	−3.85%	−3.85%	−3.85 %	0%
E_2 [MPa]	Mean	8 464	8 477	7 016	7 035	7 087	7 294
	STDV	27	271	228	229	103	201
	Rel. dif.	–	0.15%	−17.11%	−16.88%	−16.27 %	−13.82%
G_{12} [MPa]	Mean	4 336	4 355	3 900	4 026	4 042	4 068
	STDV	35	143	131	133	70	132
	Rel. dif.	–	0.44%	−10.06%	−7.15%	−6.82 %	−6.18%
G_{23} [MPa]	Mean	3 193	3 204	2 696	2 705	2 721	2 771
	STDV	15	91	84	87	51	80
	Rel. dif.	–	0.34%	−15.57%	−15.28%	−14.78 %	−13.21%
ν_{23} [–]	Mean	0.33	0.32	0.30	0.30	0.30	0.32
	STDV	0.0	0.02	0.02	0.02	0.01	0.02
	Rel. dif.	–	−3.03%	−9.09%	−9.09%	−9.09 %	−3.03%

on the voids size and not the variability on the material properties. Therefore, for a fixed void content, the uncertainty is mainly related to the material variability whereas the knock-down factor of the mean properties comes from the presence of voids.

Table 6 shows the results for the pristine SRVE and the relative difference, i.e., the knock down factor, with respect to the models considering material variability and the presence of voids.

The longitudinal Young's modulus, E_1, suffers a reduction of around 1% when the void content increases to 7% and the fiber volume fraction remains the same. This is expected, since E_1 is mostly governed by the longitudinal Young's modulus of the fibers and the fiber volume fraction which is not affected by the presence of voids, as in [47]. However, all the other elastic properties suffer a non-negligible reduction with the presence of voids, which leads to a reduction of the matrix volume fraction. For example, the reduction of the transverse Young's modulus, E_2, is around 17%.

Comparing the results between large matrix voids and inter-fiber voids, although both have similar diameter, it observed that the reduction with inter-fiber voids is lower than with matrix voids, except for E_1. To assess the effect of fiber-void intersection, a model allowing larger intersections was created. The results show lower knock-down factors for the properties dominated by the matrix, in particular E_2 and G_{23}, including a very small decrease for G_{12}, and a higher knock-down factor for E_1. Thus, it can be concluded that the position of the voids, in particular how much intersection is allowed with the fibers, affects the global elastic response of the composite. If the voids are intersected by the fibers, instead of being completely embedded in the matrix, the transverse properties are less affected, whereas the longitudinal properties dominated by the fibers, suffer a higher reduction. Interestingly, in Ref. [14] it is shown that the effect of the position of the voids on the strength of FRPs is the opposite, i.e., the strength in the presence of inter-fiber voids tends to be lower because the intersection between fiber and voids implies higher stress concentration which induce the strength reduction.

Regarding the comparison between small and large matrix voids, there is also a clear trend that the smaller the voids are, the bigger is the reduction in the mechanical properties.

The effect of voids on the elastic properties is also compared with three analytical models. To determine the minimum number of samples, n_{anal}, to run the analytical models used in this study, a contrast of hypotheses was conducted comparing different number of samples from 20 to 50 000, with $n_{anal} = 50\,000$ used as the reference value. The contrast of hypotheses showed that with a 95% of confidence it can be assumed that the mean and the STDV for all the elastic properties with 20 samples are equal to the reference value. Thus, a number of samples $n_{anal} = 20$, which is the same sample size used for the numerical analyses, is used.

Fig. 10 shows a comparison between the results obtained from computational micromechanics and the predictions of the RoM, the Mori–Tanaka mean field theory, and the CCA model for the same fiber volume fraction. Two SRVEs are considered: a pristine SRVE without defects and only considering material variability, and an SRVE with defects. The presence of voids with the RoM model can only be evaluated reducing the V_m whereas for the Mori–Tanaka and the CCA model they are assumed as a new inclusion with a dummy material. Because the analytical models do not account for the void size, the numerical results of the SRVEs with large matrix voids are selected for comparison.

For the pristine SRVE, while the predictions of the longitudinal properties are in good agreement with the numerical results (except for ν_{12} using the CCA model), the RoM, as expected, does not properly predict the transverse and shear properties, whereas the Mori–Tanaka mean field theory provides good predictions of the transverse and shear properties. Finally, the results from the CCA model are worse than the ones from Mori–Tanaka but still in good agreement with the numerical predictions except for G_{12} and ν_{12}.

Considering the presence of defects, firstly, it is important to mention that Eqs. (B.3) and (B.4) (series model) for the prediction of the transverse Young's modulus and shear modulus of the composite using the RoM are not valid in the presence of voids, as the results would lead to higher stiffness since V_m is in the denominator. In other words, with a lower V_m, which means a higher V_v, a higher E_2 or G_{12} would be obtained. Nevertheless, the predictions of the longitudinal properties remain in good agreement with the numerical results, using either the RoM, the Mori–Tanaka mean field theory or the CCA model. For the transverse and shear properties, the Mori–Tanaka mean field theory still provides the best predictions compared to the numerical model, but with a higher difference compared to the pristine results.

The CCA model is also able to capture the effect of having the voids in the matrix or within the fibers by changing the position of each phase. In that case, 3-phase CCA model is considered with the voids in the middle, embedded by the fibers, and the matrix as the outer surface. Therefore, the effect of inter-fiber voids, in that case voids completely inside the fibers, can be also considered. Using this analytical model, the same trend observed in the numerical predictions was obtained: a lower reduction of the transverse properties and a significant effect on the longitudinal properties.

Regarding the uncertainty, which is mainly dominated by the variation of the material properties, both analytical models present similar

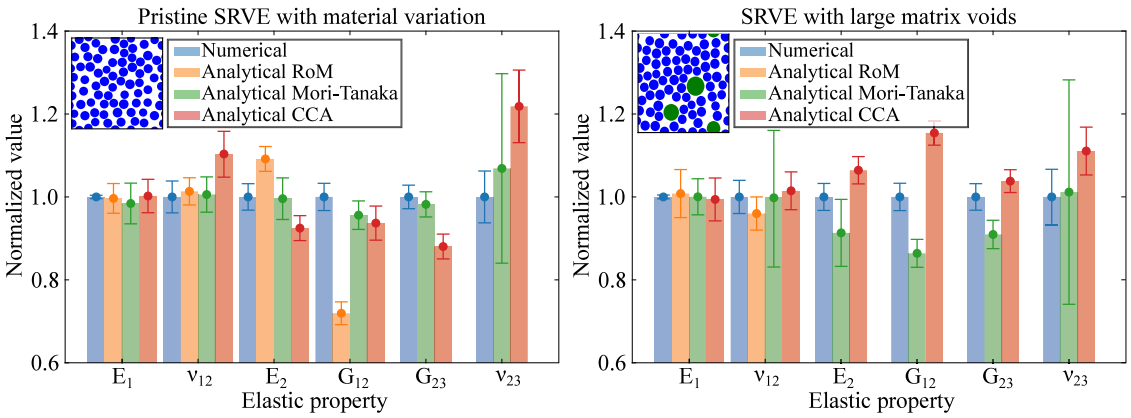

Fig. 10. Normalized elastic properties from the numerical analysis, the rule of mixtures (RoM), the Mori–Tanaka mean field theory, and the concentric cylinder assembly (CCA) of a pristine SRVE and an SRVE with large matrix voids. The error bar corresponds to one STDV. (For interpretation of the references to color in this figure legend, the reader is referred to the web version of this article.).

predictions except for E_1 and ν_{23}. Regarding E_1, the STDV obtained analytically without or with defects is much higher (more than 10 times) than the one obtained with the micromechanical model. Taking into account that E_1 is mainly dominated by the fiber properties, a higher STDV can be explained because in the micromechanical model each SRVE has different material properties for each fiber according to their corresponding normal distribution (variability from fiber to fiber as shown in Fig. 5). Thus, the different properties from fiber to fiber tends to cancel out in each SRVE. However, in the analytical models, the fiber properties only change from sample to sample inducing a higher variability between samples and, consequently, a higher STDV. A numerical analysis replicating the same conditions of the analytical models, i.e., with all fibers of each SRVE having the same randomly assigned material properties, was conducted and the STDV obtained was similar to the analytical one. Finally, it is important to note that, although there is no quantitative comparison with experimental results, the computational micromechanics modeling strategy employed here to predict the elastic properties of fiber reinforced polymers has been previously validated, e.g., Ref. [46]. Moreover, the results obtained with the presence of voids are in good agreement with the analytical models that have been already validated, incl. Mori–Tanaka mean field theory in Ref. [40] and the concentric cylinder assembly model in Ref. [41]. However, computational micromechanics provides higher flexibility in the parametrization of the SRVEs for uncertainty quantification analyses.

4.3. Parametric study of the influence of fiber and void content

The presented methodology can be used to study the influence of the input parameters (the geometry, the material variability and the presence of voids) on the mesoscale properties. This influence can be easily represented with a response surface which is a useful tool to compare the homogenized elastic properties obtained varying two of the input parameters. The previous discussed results (see Section 4.2) show that the highest effect of voids is in the transverse and shear properties. Since E_1 mainly depends on the longitudinal Young's modulus of the fibers and the fiber volume fraction, E_1 is almost independent of the V_v. Thus, Fig. 11 shows the prediction of the elastic transverse and shear moduli for different fiber (V_f) and void volume fractions (V_v) obtained numerically with the presence of large matrix voids and the relative difference between numerical predictions and analytical ones using the Mori–Tanaka mean field theory, which has been demonstrated to be the analytical model with closer predictions.

As expected, the elastic moduli are reduced with decreasing V_f. The elastic moduli governed mainly by the matrix, E_2 and G_{23}, show a pronounced reduction while increasing the V_v. However, as predicted by Tai et al. [49] in their micromechanical model with the presence of matrix microvoids, the reduction of G_{23} is more affected by the V_f rather than higher V_v. Regarding the longitudinal shear modulus G_{12}, which is more affected by the V_f rather than the V_v, the reduction due to a greater V_v is less noticeable.

The relative difference between the numerical results and the analytical Mori–Tanaka mean field theory increases with higher V_v. Regarding the V_f, the relative difference also increases with increasing V_f, although the increasing difference is less pronounced. For all the transverse and shear properties the analytical model underpredicts the elastic moduli. Nevertheless, the analytical model is able to capture the same trend obtained numerically for all the elastic properties.

The same analysis has been performed to check the effect of V_f and V_v on the uncertainty. However, no trend on the evolution of the STDV of the elastic properties with void and fiber volume fractions has been identified.

5. Conclusions

In this study, the definition of SRVEs to account for the effect of defects on the elastic properties of composite systems, including their uncertainty, is presented. An enhanced algorithm to generate the spatial distribution of the constituents in an RVE has been implemented with the ability of adding voids which have been represented as cylindrical branch-type defects aligned with the fiber direction. This RVE has been numerically simulated with a well parameterized modeling strategy, which accounts for different types of voids and materials. SRVEs are then determined for the uncertainty quantification and management of the mechanical response of composite systems with defects at the micro-scale.

Based on the elastic response of the constituents, and through the analysis of contrast of hypotheses, it is demonstrated that, as expected, the presence of voids reduces the transverse and shear elastic properties. However, for the same fiber and void volume fractions, voids completely embedded in the matrix (matrix voids) lead to higher reductions in elastic properties than inter-fiber voids of similar size, except for E_1, showing that the position of the voids affects how detrimental is their effect on the elastic properties. On the other hand, the smaller the matrix voids, the larger is the reduction in the elastic properties of the composite. Regarding the effect on the uncertainties of the meso-scale properties, it is clear that, for a fixed void content, material variability has a larger effect than the presence of voids. The material variability, in this case, is responsible for the uncertainties at the meso-scale level, while the voids are mainly responsible for the reduction of the predicted elastic properties, in particular the transverse and shear ones. Finally, the comparison with analytical models shows that the Mori–Tanaka mean field theory provides the same trends of

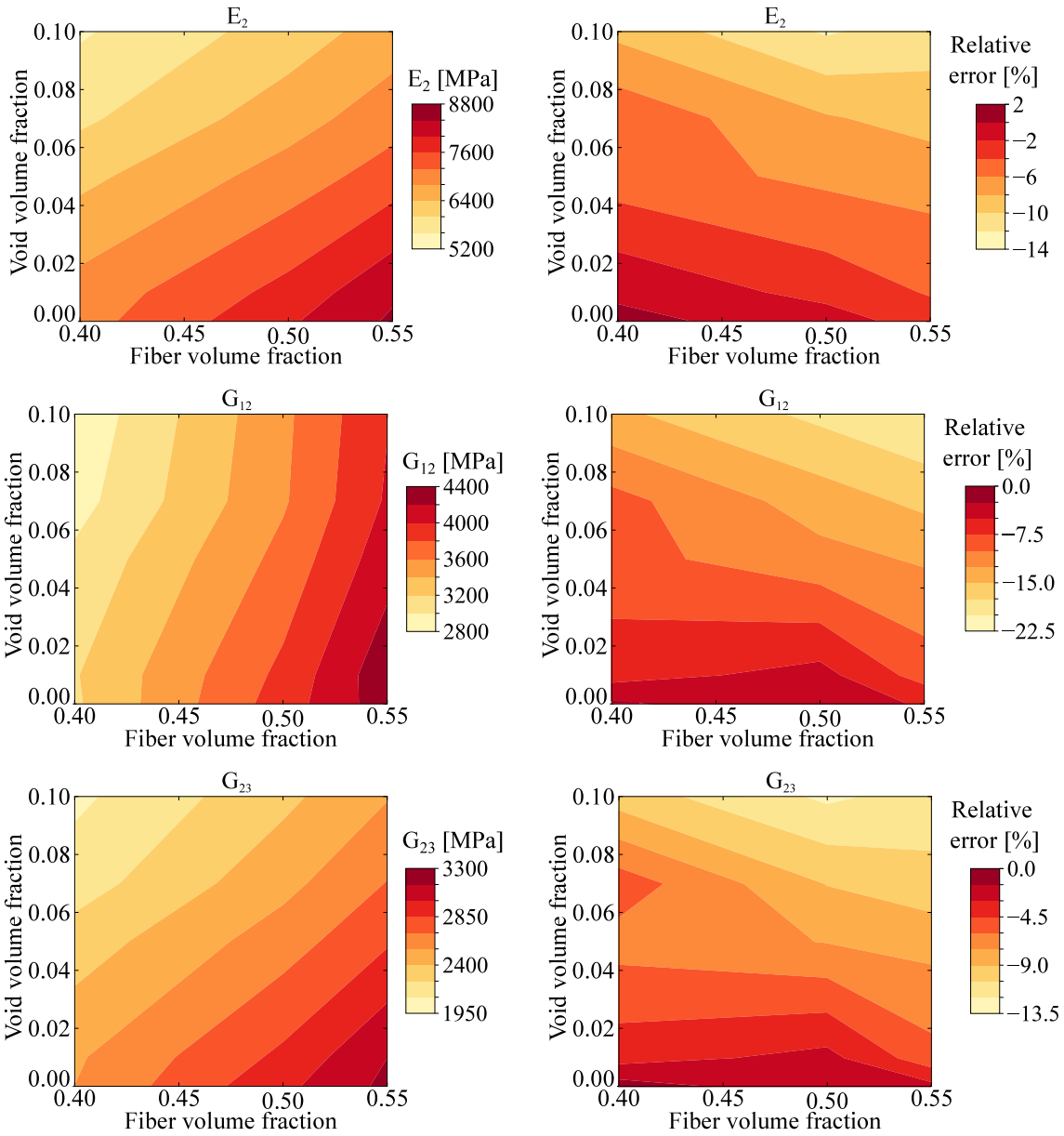

Fig. 11. Prediction of the elastic transverse and shear moduli obtained numerically with the presence of large matrix voids and the relative difference between numerical results and the analytical ones from Mori–Tanaka mean field theory. (For interpretation of the references to color in this figure legend, the reader is referred to the web version of this article.).

the numerical results for the transverse properties as a function of fiber and void volume contents. However, the relative difference between the numerical and the analytical predictions increases for high void volume fractions.

To sum up, this study shows how the added flexibility provided by computational micromechanics can aid in assessing the effect of material variability, geometric variability, as well as other microstructural effects, such as the presence of defects. Accounting for all these effects will be key in enabling multiscale reliability-based design of composite structures, linking the microstructural features with the macroscopic response and uncertainty management. Moreover, the methodology proposed herein can be extended to include the effects of other uncertainties, such as the presence of clusters of fibers or voids, and other types of defects.

CRediT authorship contribution statement

O. Vallmajó: Conceptualization, Methodology, Software, Validation, Formal analysis, Investigation, Data curation, Writing – Original Draft. **A. Arteiro:** Conceptualization, Validation, Formal analysis, Data curation, Writing – Review & Editing, Supervision. **J.M. Guerrero:** Software, Formal analysis, Writing – Review & Editing. **A.R. Melro:** Software, Formal analysis, Writing – Review & Editing. **A. Pupurs:** Conceptualization, Software, Writing – Review & Editing. **A. Turon:** Conceptualization, Validation, Formal analysis, Writing – Review & Editing, Supervision, Project administration, Funding acquisition.

Declaration of competing interest

The authors declare that they have no known competing financial interests or personal relationships that could have appeared to influence the work reported in this paper.

Data availability

No data was used for the research described in the article

Acknowledgments

OV acknowledges the support of the Catalan Government, under the Grant 2020FI B2 00110. AT and OV gratefully acknowledge the funding of the Project RTI, United States 2018-099373-B-100, co-financed by the Spanish Government (Ministerio de Economia *y* Competitividad) and the European Social Fund. AT acknowledges the Generalitat de Catalunya for the ICREA Academia prize 2022. This work has been conducted within the framework of the CAELESTIS project, funded by the European Climate, Infrastructure and Environment Executive Agency (CINEA) under grant agreement No. 101056886. Views and opinions expressed are however those of the author(s) only and do not necessarily reflect those of CINEA. Neither the European Union nor the granting authority can be held responsible for them. J.M. Guerrero would also like to acknowledge the funding of the post-doc grant Margarita Salas with reference REQ2021-A-15, financed by the Spanish "Ministerio de Universidades" and the European Union - Next GenerationEU.

Appendix A. First-order homogenization

The elastic properties of a composite material can be determined using a first-order homogenization technique. The Hooke's law for transversely isotropic materials can be defined as:

$$\begin{Bmatrix} \bar{\sigma}_{11} \\ \bar{\sigma}_{22} \\ \bar{\sigma}_{33} \\ \bar{\sigma}_{12} \\ \bar{\sigma}_{13} \\ \bar{\sigma}_{23} \end{Bmatrix} = \begin{bmatrix} C_{1111} & C_{1122} & C_{1122} & 0 & 0 & 0 \\ C_{1122} & C_{2222} & C_{2233} & 0 & 0 & 0 \\ C_{1122} & C_{2233} & C_{2222} & 0 & 0 & 0 \\ 0 & 0 & 0 & C_{4444} & 0 & 0 \\ 0 & 0 & 0 & 0 & C_{4444} & 0 \\ 0 & 0 & 0 & 0 & 0 & \frac{C_{2222}-C_{2233}}{2} \end{bmatrix} \begin{Bmatrix} \bar{\epsilon}_{11} \\ \bar{\epsilon}_{22} \\ \bar{\epsilon}_{33} \\ \bar{\epsilon}_{12} \\ \bar{\epsilon}_{13} \\ \bar{\epsilon}_{23} \end{Bmatrix} \tag{A.1}$$

where $\bar{\sigma}_{ij}$ represents the volume average of the ij stress component, C_{iijj} are the stiffness tensor components and $\bar{\epsilon}_{ij}$ is the volume average of the ij strain component. From the stiffness tensor components, the five independent engineering constants and the transverse Poisson's ratio, can be calculated as:

$$\begin{aligned} E_1 &= C_{1111} - \frac{2C_{1122}^2}{C_{2222}+C_{2233}} \\ \nu_{12} &= \frac{C_{1122}}{C_{2222}+C_{2233}} \\ E_2 &= C_{2222} + \frac{C_{1122}^2(C_{2233-C_{2222}}) + C_{2233}(C_{1122}^2 - C_{1111}C_{2233})}{C_{1111}C_{2222}+C_{1122}^2} \\ G_{12} &= C_{4444} \\ G_{23} &= \frac{C_{2222}-C_{2233}}{2} \\ \nu_{23} &= \frac{C_{1111}C_{2233}-C_{1122}^2}{C_{1111}C_{2222}-C_{1122}^2} \end{aligned} \tag{A.2}$$

where E_1 and E_2 are the longitudinal and transverse Young's moduli, G_{12} and G_{23} are the longitudinal and transverse shear moduli, ν_{12} is the major Poisson's ratio, and ν_{23} is the transverse Poisson's ratio. For a given applied far-field strain ϵ_{ij}^0, the volume average strain components can be calculated as:

$$\bar{\epsilon}_{ij} = \frac{1}{V}\int_V \epsilon_{ij} dV = \epsilon_{ij}^0 \tag{A.3}$$

and the volume average stress field as:

$$\bar{\sigma}_{ij} = \frac{1}{V}\int_V \sigma_{ij} dV \tag{A.4}$$

Therefore, since the stiffness tensor is symmetric (Eq. (A.1)), and taking into account Eq. (A.2), applying ϵ_{11}^0, ϵ_{22}^0 and ϵ_{12}^0 far-field strains is sufficient to determine the components of the stiffness tensor and, consequently, all the homogenized elastic material properties.

Appendix B. The rule of Mixtures

The Rule of Mixtures (RoM) provides reasonable values for the longitudinal stiffness (E_1) assuming that the fibers and the matrix are working in parallel:

$$E_1 = V_f E_{1f} + V_m E_m \tag{B.1}$$

where V_f is the fiber volume fraction and V_m is the matrix volume fraction, and $V_f + V_m + V_v = 1$, where V_v is the void volume fraction. E_{1f} is the longitudinal Young's modulus of the fibers, assumed transversely isotropic, and E_m is the Young's modulus of the matrix, assumed isotropic. The major Poisson's ratio (ν_{12}) can be estimated following the same assumption, as:

$$\nu_{12} = V_f \nu_{12f} + V_m \nu_m \tag{B.2}$$

where ν_{12f} is the major Poisson's ratio of the fibers and ν_m the Poisson's ratio of the matrix.

The transverse Young's modulus (E_2) can be calculated assuming that the fibers and matrix are working as springs in series:

$$E_{2,RoM} = \frac{E_m E_{2f}}{E_m V_f + E_{2f} V_m} \tag{B.3}$$

where E_{2f} is the transverse Young's modulus of the fibers. Finally, the shear modulus can be calculated as:

$$G_{12,RoM} = \frac{G_m G_{12f}}{G_m V_f + G_{12f} V_m} \tag{B.4}$$

where G_{12f} is the longitudinal shear modulus of the fibers and G_m is the shear modulus of the matrix.

Appendix C. The Mori–Tanaka mean field theory

The Mori–Tanaka mean field theory [40] account for the presence of multiple types of inclusions (here fibers and voids). In that case, for a system with unidirectional fibers with a transversely isotropic behavior and with more than one inclusion (fibers and voids), the overall elastic moduli and Poisson's ratio can be calculated as [50]:

$$\begin{aligned} p^* &= \frac{\sum_{i=1}^n \frac{V_i p_i}{p_m+p_i}}{\sum_{i=1}^n \frac{V_i}{p_m+p_i}} = G_{12} \\ \gamma_m &= \left(\frac{1}{m_m} + \frac{2}{k_m}\right)^{-1} \\ m^* &= \frac{\sum_{i=1}^n \frac{V_i m_i}{m_i+\gamma_m}}{\sum_{i=1}^n \frac{V_m}{m_i+\gamma_m}} = G_{23} \\ k^* &= \frac{\sum_{i=1}^n \frac{V_i k_i}{m_m+k_i}}{\sum_{i=1}^n \frac{V_i}{m_m+k_i}} = -\left(\frac{1}{G_{23}} - \frac{4}{E_2} + \frac{4\nu_{12}^2}{E_1}\right)^{-1} \\ l^* &= \frac{\sum_{i=1}^n \frac{V_i l_i}{m_m+k_i}}{\sum_{i=1}^n \frac{V_i}{m_m+k_i}} = 2k^*\nu_{12} \\ n^* &= \sum_{i=1}^n V_i n_i - \sum_{i=1}^n V_i \frac{(l_i-l_m)^2}{m_m+k_i} + \frac{\left[\sum_{i=1}^n V_i \frac{(l_i-l_m)}{m_m+k_i}\right]^2}{\sum_{i=1}^n \frac{V_i}{m_m+k_i}} = E_1 + 4k^*\nu_{12}^2 \end{aligned} \tag{C.1}$$

where k^*, l^*, m^*, n^* and p^* are Hill's elastic moduli [50], and the index i refers to each inclusion (i.e., fibers and voids) and m to the matrix.

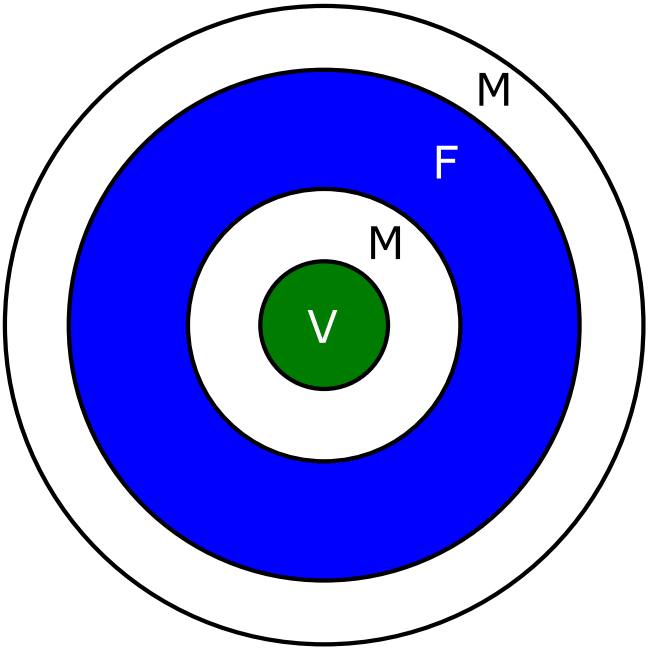

Fig. D.1. 4-phase CCA model representing UD composite with voids in the matrix phase: V – void, M – matrix, F – fiber.

The Hill's elastic moduli for an isotropic material, such as the matrix, are:

$$\begin{aligned} m_m &= p_m = G_m \\ l_m &= 2k_m\nu_m \\ n_m &= E_m + 4k_m\nu_m^2 \\ k_m &= \frac{-1}{\frac{1}{G_m} - \frac{4}{E_m} + \frac{4\nu_m^2}{E_m}} \end{aligned} \tag{C.2}$$

whereas for a transversely isotropic reinforcement, such as the fibers, they are described as:

$$\begin{aligned} m_i &= G_{i,23} \\ p_i &= G_{i,12} \\ l_i &= 2k_i\nu_{i,12} \\ n_i &= E_{i,1} + 4k_i\nu_{i,12}^2 \\ k_i &= \frac{-1}{\frac{1}{G_{i,23}} - \frac{4}{E_{i,2}} + \frac{4\nu_{i,12}^2}{E_{i,1}}} \end{aligned} \tag{C.3}$$

Appendix D. The concentric cylinder assembly model

The concentric cylinder assembly (CCA) model [41] also allows the presence of multiple phases. The micromechanical model is a straightforward extension of Hashin's [51] and Christensen and Lo's [52] models with the main novelty of its applicability to multilayered (N-phased) inclusions with transversely isotropic material properties. The composite consists of N-cylinders perfectly bonded together in which each phase (k) is homogeneous, linear elastic and with a transversely isotropic behavior. The outer (r_k) and inner radius (r_{k-1}) of each cylinder, i.e., the thickness, is determined according to each corresponding volume fraction (V_k) as:

$$V_k = \frac{r_k^2 - r_{k-1}^2}{r_N^2} \tag{D.1}$$

where $r_N = 1$ since the calculated effective elastic properties depend only on the relative dimensions of constituents. Thus, macroscopically, the composite is transversely isotropic. The problem of radial loading is solved to find the bulk modulus K_{23}, of axial loading to find E_1 and ν_{12}, of in-plane shear loading to find G_{12} and of shear loading in the plane transverse to the fibers to find G_{23}. Finally, E_2 and ν_{23} are determined using:

$$\begin{aligned} E_2 &= \frac{1}{\frac{1}{4K_{23}} + \frac{1}{4G_{23}} + \frac{\nu_{12}^2}{E_1}} \\ \nu_{23} &= \frac{E_2}{2G_{23}} - 1 \end{aligned} \tag{D.2}$$

In the present study, to account for the presence of voids, a first phase representing the voids with near zero elastic properties is embedded inside a cylinder representing the matrix. The void and matrix unit is surrounded by a cylinder which represents fibers. Finally, the final outer phase in the 4 cylinder model represents the matrix. It was found that such 4-phase CCA model (see Fig. D.1) is a more realistic representation of UD composite with voids in matrix compared to a similar 3-phase CCA model with outer phase being the fiber cylinder as the latter leads to underestimation of transverse modulus and a large overestimation of in-plane shear modulus.

References

[1] Greenhalgh E. Failure analysis and fractography of polymer composites. Woodhead, Cambridge; 2009.
[2] Mehdikhani M, Petrov NA, Straumit I, Melro AR, Lomov SV, Gorbatikh L. The effect of voids on matrix cracking in composite laminates as revealed by combined computations at the micro-and meso-scales. Composites A 2019;117:180–92.
[3] Zhou X-Y, Qian S-Y, Wang N-W, Xiong W, Wu W-Q. A review on stochastic multiscale analysis for FRP composite structures. Compos Struct 2022;284:115132.
[4] Yang P, Elhajjar R. Porosity content evaluation in carbon-fiber/epoxy composites using X-ray computed tomography. Polym-Plast Technol Eng 2014;53(3):217–22.
[5] Thomason J. The interface region in glass fibre-reinforced epoxy resin composites: 2. Water absorption, voids and the interface. Composites 1995;7(26):477–85.
[6] Drach B, Tsukrov I, Gross T, Dietrich S, Weidenmann K, Piat R, Böhlke T. Numerical modeling of carbon/carbon composites with nanotextured matrix and 3D pores of irregular shapes. Int J Solids Struct 2011;48(18):2447–57.
[7] Tserpes K, Stamopoulos A, Pantelakis SG. A numerical methodology for simulating the mechanical behavior of CFRP laminates containing pores using X-ray computed tomography data. Composites B 2016;102:122–33.
[8] Matveeva A, Garoz D, Sevenois R, Zhu M, Pyl L, Van Paepegem W, et al. Effect of intra-ply voids on the homogenized behavior of a ply in multidirectional laminates. In: IOP conference series: Materials science and engineering, vol. 406, no. 1. IOP Publishing; 2018, 012009.
[9] Stamopoulos A, Tserpes K, Prucha P, Vavrik D. Evaluation of porosity effects on the mechanical properties of carbon fiber-reinforced plastic unidirectional laminates by X-ray computed tomography and mechanical testing. J Compos Mater 2016;50(15):2087–98.
[10] Huang H, Talreja R. Effects of void geometry on elastic properties of unidirectional fiber reinforced composites. Compos Sci Technol 2005;65(13):1964–81.
[11] Zhu H, Wu B, Li D, Zhang D, Chen Y. Influence of voids on the tensile performance of carbon/epoxy fabric laminates. J Mater Sci Technol 2011;27(1):69–73.
[12] Yang P, El-Hajjar R. Porosity defect morphology effects in carbon fiber–epoxy composites. Polym-Plast Technol Eng 2012;51(11):1141–8.
[13] Scott A, Sinclair I, Spearing SM, Mavrogordato MN, Hepples W. Influence of voids on damage mechanisms in carbon/epoxy composites determined via high resolution computed tomography. Compos Sci Technol 2014;90:147–53.
[14] Hyde A, He J, Cui X, Lua J, Liu L. Effects of microvoids on strength of unidirectional fiber-reinforced composite materials. Composites B 2020;187(107844).
[15] Vajari DA, Gonzalez C, Llorca J, Legarth BN. A numerical study of the influence of microvoids in the transverse mechanical response of unidirectional composites. Compos Sci Technol 2014;97:46–54.
[16] Chambers A, Earl J, Squires C, Suhot M. The effect of voids on the flexural fatigue performance of unidirectional carbon fibre composites developed for wind turbine applications. Int J Fatigue 2006;28(10):1389–98.
[17] Hernández S, Sket F, Molina-Aldareguı J, González C, LLorca J, et al. Effect of curing cycle on void distribution and interlaminar shear strength in polymer-matrix composites. Compos Sci Technol 2011;71(10):1331–41.

[18] Mehdikhani M, Nguyen NQ, Straumit I, Gorbatikh L, Lomov SV. Analysis of void morphology in composite laminates using micro-computed tomography. In: IOP conference series: Materials science and engineering, vol. 406, no. 012010. IOP Publishing; 2018.
[19] Bodaghi M, Cristóvão C, Gomes R, Correia N. Experimental characterization of voids in high fibre volume fraction composites processed by high injection pressure RTM. Composites A 2016;82:88–99.
[20] Hyde A, Liu L, Cui X, Lua J. Micromechanics-enriched finite element modeling of composite structures with fiber waviness and void defects. In: AIAA scitech 2019 forum. 2019, p. 0694.
[21] Zhang D, Heider D, Advani SG, Gillespie J. Out of autoclave consolidation of voids in continuous fiber reinforced thermoplastic composites. In: SAMPE 2013-Long Beach. 2013, p. 16.
[22] Daggumati S, Sharma A, Van Paepegem W. Synergistic effects of microscale variabilities on the thermo-mechanical behavior of a UD CFRP ply. Int J Mech Sci 2023;242:108004.
[23] de Almeida SFM, Neto ZdSN. Effect of void content on the strength of composite laminates. Compos Struct 1994;28(2):139–48.
[24] Chu Y, Sun L, Yang X, Wang J, Huang W. Multiscale simulation and theoretical prediction for the elastic properties of unidirectional fiber-reinforced polymer containing random void defects. Polym Compos 2021;42(6):2958–72.
[25] Melro A, Camanho P, Pinho S. Generation of random distribution of fibres in long-fibre reinforced composites. Compos Sci Technol 2008;68(9):2092–102.
[26] Tavares RP, Melro AR, Bessa MA, Turon A, Liu WK, Camanho PP. Mechanics of hybrid polymer composites: analytical and computational study. Comput Mech 2016;57(3):405–21.
[27] Hill R. Elastic properties of reinforced solids: some theoretical principles. J Mech Phys Solids 1963;11(5):357–72.
[28] Dong C. Effects of process-induced voids on the properties of fibre reinforced composites. J Mater Sci Technol 2016;32(7):597–604.
[29] Sharifpour F, Montesano J, Talreja R. Assessing the effects of ply constraints on local stress states in cross-ply laminates containing manufacturing induced defects. Composites B 2020;199:108227.
[30] Vinot M, Liebold C, Usta T, Holzapfel M, Toso N, Voggenreiter H. Stochastic modelling of continuous glass-fibre reinforced plastics–considering material uncertainty in microscale simulations. J Compos Mater 2023;57(1):133–45.
[31] Vallmajó O, Cózar I, Furtado C, Tavares R, Arteiro A, Turon A, et al. Virtual calculation of the B-value allowables of notched composite laminates. Compos Struct 2019;212:11–21.
[32] Military Handbook. MIL-HDBK-17-1F: Composite materials handbook, volume 1-polymer matrix composites guidelines for characterization of structural materials. US Department of Defense.
[33] Cózar I, Turon A, González E, Vallmajó O, Sasikumar A. A methodology to obtain material design allowables from high-fidelity compression after impact simulations on composite laminates. Composites A 2020;139:106069.
[34] Tavaf V, Saadatzi M, Banerjee S. Quantification of degraded constitutive coefficients of composites in the presence of distributed defects. J Compos Mater 2019;53(18):2517–29.
[35] Mehdikhani M, Gorbatikh L, Verpoest I, Lomov SV. Voids in fiber-reinforced polymer composites: A review on their formation, characteristics, and effects on mechanical performance. J Compos Mater 2019;53(12):1579–669.
[36] Bowles KJ, Frimpong S. Relationship between voids and interlaminar shear strength of polymer matrix composites. In: International SAMPE symposium and exhibition, no. E-5825. 1991.
[37] Melro A, Camanho P, Pires FA, Pinho S. Numerical simulation of the non-linear deformation of 5-harness satin weaves. Comput Mater Sci 2012;61:116–26.
[38] ABAQUSInc. User's manual, 6.14-2. Pawtucket, RI, USA; 2014.
[39] Arteiro A, Pereira L, Bessa M, Furtado C, Camanho P. A micro-mechanics perspective to the invariant-based approach to stiffness. Compos Sci Technol 2019;176:72–80.
[40] Mori T, Tanaka K. Average stress in matrix and average elastic energy of materials with misfitting inclusions. Acta Metall 1973;21(5):571–4.
[41] Marklund E, Varna J, Neagu RC, Gamstedt EK. Stiffness of aligned wood fiber composites: effect of microstructure and phase properties. J Compos Mater 2008;42(22):2377–405.
[42] Trias D, Costa J, Turon A, Hurtado J. Determination of the critical size of a statistical representative volume element (SRVE) for carbon reinforced polymers. Acta Mater 2006;54(13):3471–84.
[43] Soden PD, Hinton MJ, Kaddour A. Lamina properties, lay-up configurations and loading conditions for a range of fibre reinforced composite laminates. In: Failure criteria in fibre-reinforced-polymer composites. Elsevier; 2004, p. 30–51.
[44] Sotiropoulos DG, Tserpes K. Interval-based computation of the uncertainty in the mechanical properties and the failure analysis of unidirectional composite materials. Math Comput Appl 2022;27(3):38.
[45] Breite C, Melnikov A, Turon A, de Morais A, Le Bourlot C, Maire E, et al. A synchrotron computed tomography dataset for validation of longitudinal tensile failure models based on fibre break and cluster development. Data Brief 2021;39:107590.
[46] Melro A, Camanho P, Pinho S. Influence of geometrical parameters on the elastic response of unidirectional composite materials. Compos Struct 2012;94(11):3223–31.
[47] Li Y, Zhou L, Zhang M, Song C. Study on the effect of void defect on mechanical properties of carbon fiber composites by finite element method. J Inst Eng (India) Ser C 2022;103(6):1433–46.
[48] González C, LLorca J. Mechanical behavior of unidirectional fiber-reinforced polymers under transverse compression: Microscopic mechanisms and modeling. Compos Sci Technol 2007;67(13):2795–806.
[49] Tai J-H, Kaw A. Transverse shear modulus of unidirectional composites with voids estimated by the multiple-cells model. Composites A 2018;105:310–20.
[50] Chen T, Dvorak GJ, Benveniste Y. Mori–Tanaka estimates of the overall elastic moduli of certain composite materials. ASME J Appl Mech 1992;59(3):539–46.
[51] Hashin Z. Analysis of composite materials—a survey. J Appl Mech 1983;50(3):481–505.
[52] Christensen R, Lo K. Solutions for effective shear properties in three phase sphere and cylinder models. J Mech Phys Solids 1979;27(4):315–30.